Removal of Cd^{2+} from aqueous solution using graphene oxide modified activate carbon derived from peanut shell

Yilu Du[1], Hui Wang[1*], Jiangtao Ji[2*], Xin Jin[2], Yang Song[2], Hao Zhang[3], Zhi Chen[4]

(1. *School of Chemistry and Chemical Engineering, Henan University of Science and Technology, Henan Luoyang, 471023, China*;
2. *College of Agricultural Equipment Engineering, Henan University of Science and Technology, Henan Luoyang, 471003, China*;
3. *Analysis and Testing Center of Liming Research & Design Institute of Chemical Industry Co., Ltd., Henan Luoyang, 471001, China*;
4. *Department of Building, Civil and Environmental Engineering, Concordia University, Montreal H3G 1M8, Canada*)

Abstract: Graphene oxide (GO) was prepared by a modified Hummers method using peanut shells and natural graphite, and graphene oxide modified peanut shells activated carbon composites (GO-AC) were synthesized by co-pyrolysis. The optimal preparation conditions of AC were screened by response surface methodology (RSM) to optimize the preparation process. The results showed that the surface of GO-AC had more micropores and larger specific surface area, increased the surface adsorption sites and had more oxygen-containing functional groups. The adsorption process was mainly based on chemisorption, and the adsorption capacity was 3.45 and 1.30 times higher than that of BC (45.16 mg/g) and AC (119.21 mg/g), respectively. After six adsorption-desorption cycle tests, the adsorption amount of Cd^{2+} by GO-AC was still as high as 89.26 mg/g, with a percentage increase of 93.5% and 365% compared to BC (19.18 mg/g) and AC (46.13 mg/g), respectively, with good reusability. The research can provide a useful reference for the high value-added conversion of waste biomass, and GO-AC loading modified with significant adsorption of Cd^{2+} has good potential for application as a novel and low-cost adsorbent.

Keywords: graphene oxide-modified biochar, response surface optimization, adsorption, heavy metal
DOI: 10.25165/j.ijabe.20231605.8046

Citation: Du Y L, Wang H, Ji J T, Jin X, Song Y, Zhang H, et al. Removal of Cd^{2+} from aqueous solution using graphene oxide modified activate carbon derived from peanut shell. Int J Agric & Biol Eng, 2023; 16(5): 226–235.

1 Introduction

Earlier this decade, with the accelerated growth of the heavy metal processing, electroplating, and tanning sectors, an increasing number of heavy metal pollutants have been released directly or indirectly into natural water bodie[1]. Because of the high solubility and biological characteristics of heavy metal ions in aquatic environments, the refractory degradation and high accumulation of these ions in organisms can cause serious and irreversible harm to biological systems and communal health. To resolve the issue of heavy metal pollution, there are several effective ways to remove the heavy metals in wastewater, and it is chemical precipitation, adsorption, membrane separation, and electrochemical techniques, have been developed. Due to its high effectiveness, inexpensive cost, low secondary pollution production, promoteability, and adaptability, the adsorption method has drawn considerable interest in the management of heavy metal pollution. Biochar has been studied as a low-cost alternative adsorbent due to its porous structure, surface functional groups, low cost, energy savings, and biomass reuse capabilities; thus, biochar has great market potential as an adsorbent, especially when applied to remove heavy metals from heavy metal polluted wastewater[2,3]. At present, a large amount of agricultural waste in China cannot be properly disposed of, and it is often placed in open environments or is directly incinerated, which not only causes air pollution but also wastes resources. Large amounts of agricultural waste are converted into biochar that can adsorb heavy metals that can be modified to prepare new adsorbed heavy metal materials that effectively utilize agricultural waste resources and solve the environmental pollution problems[4,5]. Studying how to turn agricultural waste into an adsorbent that can effectively remove heavy metals is therefore extremely valuable and important from a practical standpoint.

The physicochemical characteristics of biochar, for instance, certain surface functional groups, surface area, and pore volume are important influencing factors in its adsorption performance. Sessa et al. selected pine bark to prepare biochar and activated it through chemical and physical activated it through physical and chemical means[6]; the researchers found that after chemical activation, the biochar with a higher specific surface area and better toluene adsorption performance, which increased by 38% compared to the adsorption performance before chemical activation. In the experiment of Herath et al.[7], fir wood was used to make charcoal, which was then KOH activated; the researchers discovered that after KOH activation, the pore capacity of fir-based biochar considerably increased and the specific surface area rose three-fold, and it had better adsorption effects on Cd^{2+}, Pb^{2+} and Cr^{6+}. The KOH activation process was accompanied by many chemical reactions, and the

Received date: 2022-11-22 **Accepted date:** 2023-05-11
Biographies: Yilu Du, Postgraduate, research interest: soil heavy metal pollution remediation, Email: Yilu0817@163.com; **Xin Jin**, Associate Professor, research interest: vegetable production mechanization, Email: jx.771@163.com; **Yang Song**, Postgraduate, research interest: agricultural biological environment and energy theory and technology, Email: sy1016722800@163.com; **Hao Zhang**, Engineer, research interest: soil testing and evaluation，Email: 1352009076@qq.com; **Zhi Chen**, Professor, research interest: environmental pollution control, Email: zhichen@alcor.concordia.ca.

***Corresponding author: Hui Wang**, Professor, research interest: soil pollution remediation. School of Chemistry and Chemical Engineering, Henan University of Science and Technology, Luoyang 471023, China, Tel: +86-15037938700, Email: wanghui_peony@163.com; **Jiangtao Ji**, Professor, research interest: modern agricultural equipment and intelligent technology. College of Agricultural Equipment Engineering, Henan University of Science and Technology, Luoyang 471003, China, Tel: +86-13721688350, Email: jjt0907@163.com.

intermediate products generated, such as K_2O, KOH and K_2CO_3, would combine with C in a reaction that would generate a lot of gas and encourage the growth of further pore structures[8]. Additionally, during activation, KOH might interact with functional groups in biomass that contain oxygen. Therefore, KOH activation is a viable biochar modification strategy.

However, chemical activation cannot significantly increase the functional mass of the biochar surface. To improve the efficiency of contaminant removal, the surface functional groups need to be further explored. Many studies in recent years have shown that combining traditional biochar technology with other emerging technologies, such as biotechnology and nanotechnology, can synthesize biochar-based materials with adjacent hydrophilic functional groups (engineered biochar) and enhance the organic pollutant adsorption capacity[9-11]. Graphene oxide (GO) is a two-dimensional (2D) nanomaterial that has carbon atoms arranged in a hexagonal honeycomb structure and significant mechanical and thermal properties, a high specific surface area, and a significant number of functional groups containing oxygen; GO has other characteristics that are widely used in catalysts, fillers, functional hybrid materials, energy conversion, and other fields[12-14]. According to reports, GO is an effective adsorbent for a variety of environmental pollutants, including heavy metal ions[15]. Arvas et al. prepared S, N, and Cl-doped graphene oxide electrodes using a one-step method as a high-capacitance supercapacitor electrode material with high area capacitance values[16]. Liu et al. made a hydrophilic and antibacterial bifunctional membrane with quaternary ammonium salt as a membrane modifier on the graphene oxide's surface and found that the modified membrane had stronger hydrophilicity and significantly improved the loss of antibacterial substances on the membrane surface[17]. Bao et al. coupled Fe_3O_4/SiO_2 with GO through a coupling agent to prepare a new type of magnetic graphene oxide for removing Cd(II) and Pd(III) from wastewater, which was found to have good adsorption and reproducibility[18]. Graphene oxide layers were found to produce van der Waals forces in aqueous media that facilitated agglomeration, potentially reducing adsorption capacity and making the recovery process more challenging.

Based on the previous literature, it was determined that combining this new nanomaterial with existing biochar materials to prepare a new type of nanocomposite can not only enhance the biochar's capacity for adsorption and avoid the accumulation of graphene oxide but also reduce the application cost of carbon nanocomposites. At present, studies on the adsorption effect of Cd^{2+} heavy metals on graphene oxide-modified biochar are not available. Therefore, biochar was prepared from peanut shell agricultural waste, and the optimal preparation conditions for KOH-activated biochar were determined by response surface optimization (RSM), simplifying the screening times and optimizing the preparation process. A novel GO-supported activated biochar (GO–AC) was prepared by an improved Hummers-impregnation-copyrolysis method, which allowed Cd^{2+} adsorption; then, the GO–AC sample surface areas were characterized by SEM, FTIR, XPS, and BET to evaluate the adsorption behavior of Cd^{2+} on novel carbon-containing nano load materials. Adsorption kinetics, adsorption isotherms, and adsorption-affecting factors (i.e., pH, ionic strength) were studied. In addition, the regenerative properties and adsorption mechanism of GO–AC was determined to gain insight into the adsorption behavior. This study is a helpful resource for the value-adding procedure of converting waste biomass.

2 Materials and methods

2.1 Materials

Peanut shells are taken from a farm in Luoyang, Henan Province, China (the farm center coordinates are 112°27'37.93"E and 34°56'64.43"N). HCl (hydrochloric acid), NaOH (sodium hydroxide), P_2O_5 (phosphorus pentoxide), $K_2Cr_2O_7$ (potassium dichromate), $NaNO_3$ (sodium nitrate), $K_2S_2O_8$ (potassium persulfate), H_2O_2 (hydrogen peroxide), H_2SO_4 (concentrated sulfuric acid), and experimental drugs such as $KMnO_4$ (potassium permanganate) are provided by Shanghai Aladdin Biochemical Technology Co. All experimental drugs used in this experiment are analytical pure, and the water used in the experiment is pure Wahaha water.

2.2 Preparation of BC, AC, and GO–AC

2.2.1 Preparation of GO

A modified Hummers preparation process was used to prepare graphene oxide[19]. Mix 2.00 g of graphite and 1.00 g of $NaNO_3$ and place in a 500 mL beaker. Under ice water bath conditions, add 45 mL of sulfuric acid (98%). And at a temperature below 10°C, slowly add 6.00 g of $KMnO_4$ and 1.00 g of $NaNO_3$. After vigorous agitation for 2 h under ice bath conditions, the mixture was placed at 30°C for another 30 min. Afterward, the mixture was thinned out with 100 mL of deionized water, heated to 95°C, and maintained at this temperature for 30 min. 10 mL of H_2O_2 (30%) solution was added after the suspension had reached 60°C and agitated continuously for 2 h at room temperature. The precipitate was then cleaned and rinsed with deionized water and 5% HCl until the pH of the supernatant reached 7. The prepared GO was sonicated, vacuum-dried at 65°C, and then put in a tight bag.

2.2.2 Preparation of biochar

The peanut shells were thoroughly cleaned with deionized water to get rid of contaminants, dried, ground into a powder, and then kept in a sealed container for future use.

The pretreated peanut shells were placed in a vacuum tube furnace and maintained warm for 2 h before being cooled to room temperature after being heated to 350°C at a rate of 10°C/min. To get removal of ash, the shells were submerged in HCl (0.1 mol/L) and washed with ultra-pure water to reach pH neutrality, filtered, and then dried for 24 h at 80°C. After grinding, pass through a 0.1 mm sieve and set aside in a sealed bag.

Preparation of KOH-activated peanut shell biomass carbon (AC): KOH was mixed with previously prepared biochar (BC) in 100 mL of deionized water with a carbon-based mass ratio of 2:3, and then the mixture was shaken for 5 h at 150 r/min, then dried for 24 h at 80°C in drying oven. In a vacuum tube furnace, the mixture was then heated to 700°C at a rate of 10°C/min and maintained for 2 h. After cooling the mixture to room temperature, activated biochar was created (AC).

2.2.3 Preparation of GO–AC

0.20 g graphene oxide (GO) was added to 50 mL of deionized water and then stirred at 250 r/min for 1 h; next, 4.00 g of activated biochar (AC) was added, and the sample was placed in an ultrasonic reactor with an output frequency of 20 kHz to stir the suspension at pulse intervals of 12 min. The sample was sonicated for 1 h and then placed in a freeze dryer for 24 h. The dry mixture was heated in a vacuum tube furnace at a rate of 5°C/min until it reached 180°C. It was then held at that temperature for 2 h before being cooled to ambient temperature to produce activated biochar that was modified with graphene oxide (GO–AC).

2.3 Characterization methods

SEM was used to compare the shape and surface features of the sample prior to and following alteration (JSM-5610LV type). The sample was also scanned in the 400-4000 cm^{-1} spectrum using a Fourier infrared spectrometer (Nicolet 5700 Spectrometer), and the resulting characteristics were supplemented with X-ray photoelectron spectra (Perkin-Elmer PHI 550 ESCA/SAM) to verify the surface group changes in biochar before and after modification. The specific pore size and surface area structure parameters of the biomass carbon before and after alteration were measured using the specific surface area and porosity analyzer (ASAP 2020 V 4.03 type).

2.4 RSM experimental design

The central composite design (CCD) using the response surface method (RSM) determines the optimal test response value with the least amount of trials. Cd^{2+} was determined by the biochar activation temperature (*A*), activation time (*B*), and carbon-to-alkali ratio (*C*). Three process parameters affected *Qe*, and the optimal preparation conditions (*Y*) for AC adsorption of Cd^{2+} were optimized using 3 variables and 3 levels. Table 1 lists the overall and particular experimental outcomes. The analysis of variance (ANOVA) was used to assess the model's accuracy and the importance of the process parameters[20]. Equation's quadratic polynomial model was used to calculate the AC to Cd^{2+} adsorption efficiency response value (1).

$$Y = \alpha_0 + \sum_{i=1}^{n} \alpha_i x_i + \sum_{i=1}^{n} \alpha_{ii} x_i^2 + \sum_{i=1}^{n-1} \sum_{j=i+1}^{n} \alpha_{ij} x_i x_j \quad (1)$$

where, Y is the response variable; α_0 is a constant; α_i, α_{ii}, and α_{ij} are linear, squared, and mutual constants, respectively; and x_i and x_j are arguments.

Table 1 Energy-dispersive X-ray spectroscopy (EDS) analysis of the surface areas of BC, AC, and GO–AC

Biochars	Elements	Weight percentage/%	Atomic percent/%	O/C%
BC	C	85.76	92.32	8.11
	O	6.96	5.62	
	Mg	0.20	0.11	
	Si	0.14	0.06	
	K	4.45	1.47	
	Ca	0.98	0.31	
AC	C	66.73	86.54	7.41
	O	4.95	4.82	
	Mg	0.34	0.22	
	K	18.17	7.24	
	Ca	1.30	0.50	
GO–AC	C	74.66	82.08	26.13
	O	19.51	16.10	
	Mg	0.38	0.21	
	K	0.74	0.25	
	Ca	0.31	0.10	

2.5 Adsorption experiment

Default experimental conditions: Two 0.0521 g cadmium chloride ($CdCl_2$) are dissolved in 1000 mL of ultrapure water to prepare a Cd^{2+} (1000 mg/L) stock solution. The stock solution is diluted in batch tests to produce varying Cd^{2+} concentrations. The pH is adjusted using prepared 0.1 mg/L HNO_3 and NaOH. The reaction was controlled by shocking at 150 r/min for 0.5-12 h using an air bath thermostatic shock chamber (25°C±1°C); each Erlenmeyer flask is sealed with a sealing film during the shock to reduce the influence of the actual environment on the solution.

2.5.1 Kinetic experiments

A 30 mL Cd^{2+} solution is made with a 100 mg/L Cd^{2+} concentration, a pH of 6.0, and a temperature of 25°C. 0.01 g of biochar is weighed in an Erlenmeyer flask, shaken for 0.25 h, 0.5 h, 1 h, 2 h, 3 h, 4 h, 6 h, 8 h, 12 h, and 24 h, filtered and the concentration of Cd^{2+} in the solution was determined.

2.5.2 Isothermal adsorption

The concentrations of 30 mL of Cd^{2+} solution adjusted to pH 6.0 when the temperature was set to 25°C were 30, 60, 80, 100, 120, 150, 180, and 200 mg/L. 0.01 g of biochar was weighed in an Erlenmeyer flask, shaken for 2 h, and filtered to ascertain the solution's Cd^{2+} concentration.

2.5.3 Effect of pH on adsorption effect

Prepare 30 mL of Cd^{2+} solution with a concentration of 100 mg/L. The Cd^{2+} solutions' pH level was modified to 2.0, 3.0, 4.0, 5.0, 6.0, and 7.0, and the temperature was set to 25°C. 0.01 g of biochar was weighed in an Erlenmeyer flask, shaken for 2 h, and filtered to ascertain the solution's Cd^{2+} concentration.

2.5.4 Effect of ionic strength on adsorption effect

A concentration of 30 mL was formulated as a 100 mg/L Cd^{2+} solution and a pH adjustment of 6 was made. 0.001, 0.005, 0.01, 0.05, 0.1, 0.5 and 1 mol/L NaCl solutions were added to the solution at a temperature of 25°C. 0.01 g of biochar was weighed in an Erlenmeyer flask, shaken for 2 h, and filtered to ascertain the solution's Cd^{2+} concentration.

2.5.5 Adsorption-regeneration cycle experiments

It was chosen to use 0.5 mol/L HCl as a desorption agent. A concentration of 30 mL was formulated as a 100 mg/L Cd^{2+} solution with an adjustable pH of 6.0 and a temperature of 25°C before accurately weighing 0.01 g of biochar in an Erlenmeyer flask, shaking for 2 h, and collecting filtrate for testing. The material that had been adsorbed was put into an Erlenmeyer flask with 100 mL of HCl for desorption for 12 h before being vacuum ejected and washed with deionized water to achieve pH neutrality. The sample was put in a vacuum oven and heated to 60°C for drying. An identical procedure for performing 5 adsorption-desorption experiments was used.

2.6 Data Processing and Analysis

Using an Inductively Coupled Plasma (ICP) spectrometer, the remaining Cd^{2+} concentration in the solution was determined. The adsorption capacity of the adsorbent being tested (*Qe*, mg/g) is determined by the subsequent equation:

$$Qe = \frac{[C_0 - C_e]}{m} V \quad (2)$$

where, C_0 is the initial concentration of cadmium solution, mg/mL; *Ce* is the concentration of cadmium solution after adsorption, mg/g; *V* is the volume of cadmium solution taken before adsorption, mL; and *m* is the quantity of biochar added, g.

Origin 8.0 was used for mapping, and Excel 2019 was used for data processing.

3 Results and discussion

3.1 Characterization of BC, AC, and GO–AC materials

3.1.1 SEM-EDX analysis

The scanning electron microscope (SEM) image shows the surface topography of BC, AC, and GO–AC. From Figure 1, it can be seen that the surface of BC (Figure 1a) is smooth, and after KOH activation, the surface of AC (Figure 1b) has different degrees of

etching and becomes a coarser, more finely fragmented material that is porous and loose, with honeycomb-like structures, a larger specific surface area, and more pore structures. After being modified with graphene oxide, there are obvious changes, and the surface of GO–AC (Figure 1c) is fluffy with wrinkled sheets and an overall smooth sheet exhibiting an A-layered structure with curved edges and a transparent flocculent structure with folds; the sample also has good flexibility, which is in line with previous studies[21]. The modified GO–AC has a high specific surface area, providing an efficient adsorption site and a place for subsequent loads of biomass charcoal.

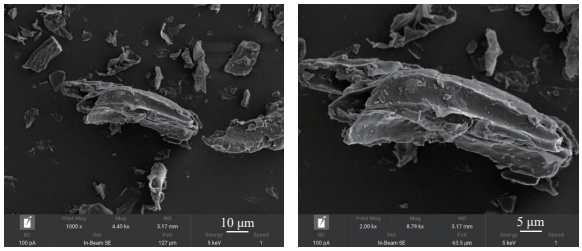

a. BC

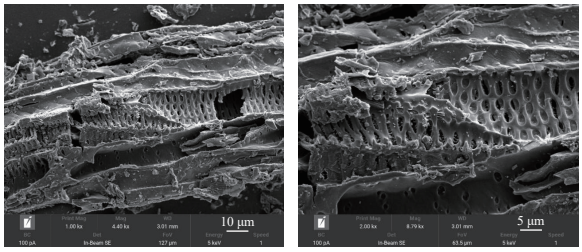

b. AC

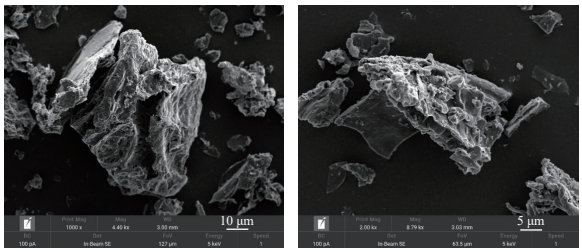

c. GO–AC

Figure 1 Scanning electron microscopy of BC, AC, and GO–AC

3.1.2 FT-IR spectroscopy

The functional groups of the BC, AC, GO–AC, and GO–AC with Cd^{2+} surfaces were determined by FT–IR technology, and the results are shown in Figure 2. Multiple adsorption peaks appear in the spectra of BC, AC, and GO–AC, indicating that the material is relatively complex. GO–AC has more feature peaks, indicating that it has more functional groups on its surface. The characteristic peak at 3423 cm^{-1} is the O-H telescopic vibration, the characteristic peak at 1598 cm^{-1} is the aromatic structure C=C telescopic vibration, and the characteristic peak at 1480 cm^{-1} is the aliphatic C-H vibration. The spectra of BC and AC have no significant peaks between 1000 and 1480 cm^{-1}. The new peak appearing in the spectrum at 491 cm^{-1} is related to the expansion and contraction vibrations of C-O and C-H. Unlike BC and AC, GO–AC has new strong peaks at 1082 cm^{-1} and 780 cm^{-1} associated with the stretching of C-O-C and aromatic compounds, respectively. In conclusion, the adsorption peaks of C-O-C, C-O, C-H, and aromatic compounds have changed after the modification, confirming that the surface functional groups of graphene oxide succeeded in embedding in the composites during the tube furnace pyrolysis. After GO–AC adsorbed Cd^{2+}, the oxygen-containing functional group changed, in which the wavelength of the C-O-C group shifted after adsorption of Cd^{2+} from 780 cm^{-1} to 791 cm^{-1} and then to 1082 cm^{-1}. The C-O location was shifted to 1097 cm^{-1}, and there was a considerable decrease in the intensity of the telescopic vibration, showing that the oxygen-containing functional groups were engaged in the adsorption process.

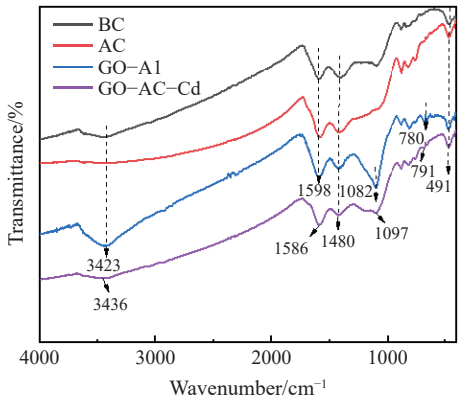

Figure 2 FT–IR spectra of BC, AC, and GO–AC

According to Table 1 and an X-ray spectroscopy (EDS) analysis, C and O are the main constituent elements of BC, AC, and GO–AC. After KOH activation, a slight decrease in C and O in AC, while the KOH-modified retention of K elements increased the amount of modified biomass carbon K. After GO loading, the O content of the GO–AC loading material increased significantly. The results show that C and O constitute the bulk of these three biochar materials. The ratios of oxygen content to carbon content (O/C) of BC, AC, and GO–AC were 8.11, 7.41, and 26.13, respectively. Obviously, the oxygen content ratio of GO–AC was much higher than those of BC and AC, suggesting the introduction of more oxygen-containing functional groups, such as C=O and C-O.

3.1.3 XPS analysis

To further understand its chemistry, we performed XPS (X-ray photoelectron spectroscopy) analyses of the BC, AC, GO–AC, and GO–AC with Cd^{2+} materials, and the results are shown in Figure 3. The XPS measurement spectrum of GO–AC–Cd^{2+} showed a significant peak at 408.0 eV, corresponding to the Cd 3d orbital. This finding suggests that Cd^{2+} was successfully adsorbed on biochar after exposure to GO–AC. Additionally, the C1s band before and after adsorption of Cd^{2+} before and after GO–AC was studied. As shown in Figure 3b, three different bands centered at 284.2 eV, 284.9 eV, and 286.7 eV were observed in the C-C/C=C, C=O, and C-O moieties of GO-AC, in correspondence with each other. XPS spectra of C1s from GO-AC with loading of Cd^{2+} (Figure 3c) clearly show four different spectral bands: C–C/C=C (283.2 eV), C–O (284.3 eV), C=O (286.1 eV), and O–C=O (291.1 eV). According to XPS, a Cd 3d feature peak at 408.0 eV and a Cd 3p feature peak at 617.0 eV appeared after the adsorption of Cd^{2+} by GO–AC, indicating that Cd^{2+} was adsorbed on the material surface. Among them, as shown in Figure 3d, the characteristic peaks of Cd 3d at 408.0 eV were found at 405.5 eV and 412.1 eV for Cd $3d_{5/2}$ and Cd $3d_{3/2}$, which proved that the valence state of Cd ion is positive divalent. The characteristic peaks of the two curves at Cd $3d_{5/2}$ after split-peak fitting correspond to $Cd(OH)_2$ and $CdCO_3$, i.e., Cd^{2+} is present in the form of precipitation on GO–AC, indicating that GO–AC removes Cd^{2+} from the solution by surface compounding and surface-induced precipitation. Generally, the binding energy of Cd $3d_{5/2}$ is 405.0 eV and that of Cd $3d_{3/2}$ is 411.7 eV, while the binding energies of both

Cd $3d_{5/2}$ (405.5 eV) and Cd $3d_{3/2}$ (412.1 eV) were increased in this study, indicating that the adsorption process appears to involve the complexation of oxygen-containing functional groups with Cd^{2+} to form Cd -R bond (R is -COO, -CO, etc.).

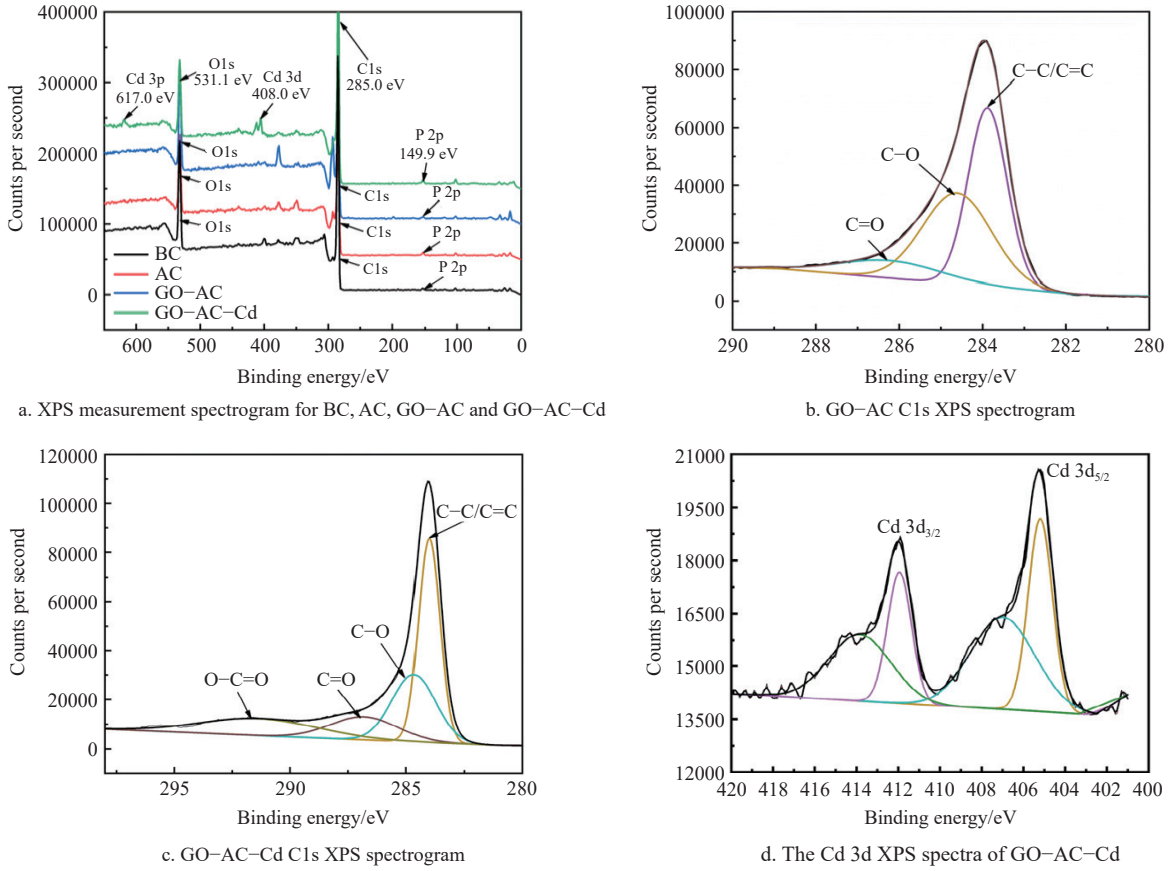

a. XPS measurement spectrogram for BC, AC, GO−AC and GO−AC−Cd

b. GO−AC C1s XPS spectrogram

c. GO−AC−Cd C1s XPS spectrogram

d. The Cd 3d XPS spectra of GO−AC−Cd

Figure 3 XPS Spectrogram

The XPS results suggest that the differences between GO–AC and GO–AC–Cd^{2+} may be the result of the introduction of oxygen-containing functional groups, which enhance the adsorption capacity. The FT-IR and XPS spectra show that GO was successfully linked to the surface of the biochar, adding more sites for Cd^{2+} to bind.

3.1.4 BET

The surface area, pore volume, and average aperture of BC, AC, and GO–AC are listed in Table 2. As shown in Table 2, GO-AC BET surface area (1719.40 m^2/g) is greater than those of BC (780.90 m^2/g) and AC (1095.79 m^2/g), which explains the successful coupling of graphene oxide on AC and the increasing surface area of GO–AC. The pore volume and aperture of GO–AC are smaller than those of BC and AC. This phenomenon may be due to the immersion of AC in graphene oxide solution during the preparation of GO–AC, which changes the pore structure of AC. In addition, changes in certain functional group ratios may limit N_2 in certain pore networks, resulting in changes in the pore volume distribution[22]. The pore volume and specific surface area of AC are higher than those of BC, which may be due to the addition of more pore structures during activation. Pore diameters of BC, AC, and GO-AC on average are 4.65 nm, 5.48 nm, and 3.49 nm, respectively, which means that all three biochar materials have predominantly medium-sized pores.

Table 2 Specific surface area, total pore volume, and average pore size of BC, AC, and GO–AC

Biochars	Specific surface area/$m^2 \cdot g^{-1}$	Pore volume/$m^3 \cdot g^{-1}$	Average pore size/nm
BC	780.90	0.34	4.65
AC	1095.79	0.48	5.48
GO–AC	1719.40	0.27	3.49

3.2 Analysis of the activated carbon preparation process based on response surface optimization

The regression equation was constructed using the full-factor three-level RSM model center composite design (CCD) by considering the biochar activation temperature (A), activation time (B), and carbon-base ratio (C) to be the independent variables. The adsorption amount of Cd^{2+} was the dependent variable, the experimental results were analyzed by quadratic multiple regression, and the response function model formula Equation (3) was established. Equation (3) is a quadratic model representing the Cd^{2+} adsorption value Qe.

$$Q_e = 134.81 + 25.92A + 14.16B + 6.30C - 11.50AB + 10.53AC + 4.05BC - 53.92A^2 - 11.16B^2 - 8.18C^2 \quad (3)$$

ANOVA determined the suitability of the model (Table 3)[23]. The findings demonstrate that the model was a good fit and was accurate in describing the link between the experimental and predicted values of Cd^{2+} adsorption. Factors A, B, and C all had p values under 0.05 among the selected adsorption parameters, indicating that they were significant within a 95% confidence interval and substantially correlated with the Cd^{2+} adsorption efficiency. In addition, the high deterministic coefficient that was derived by fitting the quadratic model (R^2=0.9802) meant that the model fit the data well enough to describe 98.02% of the change. Only 1.78% of the adjusted change did not apply to the model, as indicated by the adjusted R^2 score (0.9624) being near to R^2

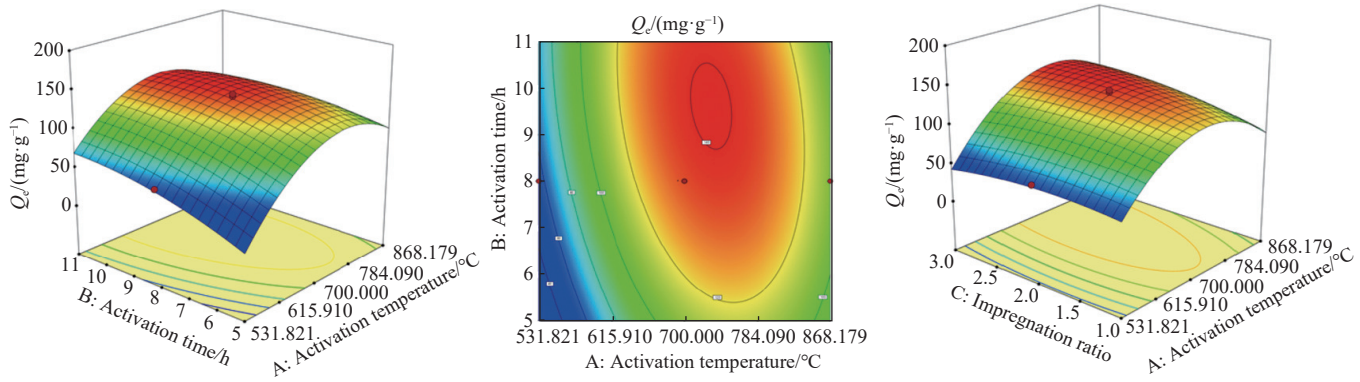

a. Effect of activation time and temperature on adsorption capacity in stereogram

b. Effect of activation time and temperature on adsorption capacity

c. Effect of impregnation ratio and temperature on adsorption capacity in stereogram

d. Effect of impregnation ratio and temperature on adsorption capacity

e. Influence of impregnation ratio and time on adsorption capacity in stereogram

f. Influence of impregnation ratio and time on adsorption capacity

Figure 4 3D surface plot and contour plot of the response of different variables to AC adsorption of Cd^{2+}

(0.9802). The 3D surface plot and contour plot of the response of different variables to AC adsorption of Cd^{2+} are shown in Figure 4.

Table 3 ANOVA results and significance of the RSM model

Source	Sum of squares	df	Mean square	*F*-value	*p*-value	
Model	14 268.57	9	1585.4	55.1	< 0.0001	significant
A	3244.26	1	3244.26	112.76	< 0.0001	
B	2739.17	1	2739.17	95.2	< 0.0001	
C	541.66	1	541.66	18.83	0.0015	
AB	3.7428E+02	1	3.74E+02	13.01	0.0048	
AC	313.75	1	313.75	10.9	0.008	
BC	131.06	1	131.06	4.56	0.0586	
A^2	5237.77	1	5237.77	182.05	< 0.0001	
B^2	1796.21	1	1796.21	62.43	< 0.0001	
C^2	963.92	1	963.92	33.5	0.0002	
Residual	287.72	10	28.77			
Lack of Fit	197.91	5	39.58	2.2	0.2031	Not significant
Pure Error	89.8	5	17.96			
Cor Total	14 556.28	19				

Note: R^2 = 0.9802; adjusted R^2 =0.9624; predicted R^2 =0.8839.

3.3 Adsorption experiment

3.3.1 Adsorption kinetics experiments

To investigate the impact of contact time on Cd^{2+} adsorption on GO-AC, adsorption kinetics experiments were performed. The kinetic curve of the adsorption amount of Cd^{2+} by BC, AC, and GO–AC changed with the adsorption time, as shown in Figure 5a, and the parameters of the adsorption kinetic model fitting results are shown in Table 4. With increasing time, the three kinds of biomass charcoal were rapidly adsorbed in the range of 0-1 h, the rate slowed down at 1-2 h, and adsorption saturation was reached at 2 h. These outcomes came about as a result of the biochar's surface having a lot of active sites at the start of the process, which can quickly bind to Cd^{2+}. Subsequently, the active site was saturated, the diffusion of Cd^{2+} to the interior was subjected to great resistance, and gradually attained adsorption equilibrium[24]. The adsorption of GO–AC reached 155.96 mg/g at 2 h, exceeding 245% and 31.8% of the adsorption of BC and AC, respectively; that is, the adsorption was greater than BC (45.16 mg/g) and AC (119.21 mg/g) by factors of 3.45 and 1.30, respectively, and the adsorption effect of GO–AC was always greater than those of BC and AC. This phenomenon may be caused by the introduction of oxygen-containing functional groups, which are substances such as hydroxyl groups that facilitate the provision of more surface adsorption sites.

Table 4 shows that the adsorption of Cd^{2+} by the three biochars fits two kinetic equations at the same time, but the R^2 of the quasi-secondary kinetics is higher than 0.95, which is more inclined to 1 than the R^2 of the quasi-primary kinetics, and the maximum theoretical adsorption amount is *Qe*, which is substantially closer to the real amount of adsorption. This demonstrates that the three biochars are more consistent with the quasi-secondary kinetic model and that chemical adsorption is the primary mechanism for Cd^{2+} adsorption. The R^2 of both models, however, was higher than 0.9, suggesting that there may be both physisorption and chemisorption involved in the adsorption of BC, AC, and GO-AC on Cd^{2+}. Among them, the k value of GO–AC is the largest, demonstrating that following GO loading, biochar has a greater adsorption rate per unit time and unit mass than BC and AC.

3.3.2 Isothermal adsorption experiment

Figure 5b shows the Langmuir and Freundlich adsorption isotherms of the three biochar materials, with the adsorption coefficients shown in Table 5. The R^2 values of the Langmuir model (0.9423, 0.9372, and 0.9749) and the Freundlich model (0.9184, 0.9063, and 0.9229) are both greater than 0.90, demonstrating that

both models are capable of adequately describing the Cd^{2+} adsorption by biochar.

The maximum adsorption capacities of BC, AC, and GO-AC on Cd^{2+} are calculated using the Langmuir model and are calculated to be 44.81 mg/g, 126.11 mg/g, and 169.96 mg/g, respectively, which are similar to the actual adsorption date. GO–AC has a higher theoretical adsorption amount. It could be a result of GO-AC's greater specific surface area, ability to produce more active groups, and capacity to provide more surface sites. When the K_L parameter value in the Langmuir model is between 0 and 1, it indicates that the reaction is easy to carry out[25]. From Table 5, as can be shown, the K_L parameters of the three kinds of biomass carbon are 0.0222 L/mg, 0.0233 L/mg· and 0.0388 L/mg, respectively. This finding shows that the adsorption process of the three kinds of biomass carbon is relatively easy to carry out, and single-layer adsorption and nonuniform surface adsorption exist simultaneously in the process of adsorption of Cd^{2+}, but single-molecular-layer adsorption dominates.

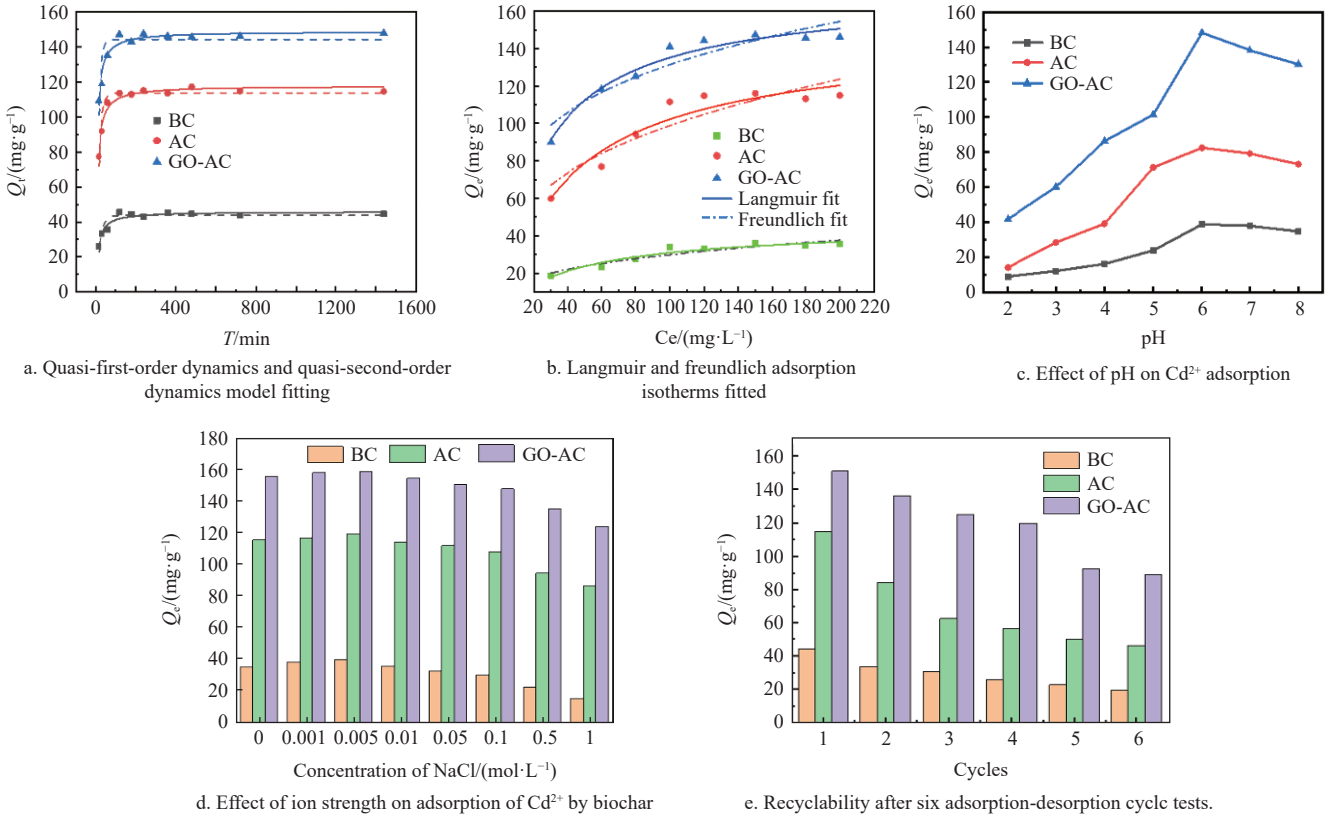

a. Quasi-first-order dynamics and quasi-second-order dynamics model fitting

b. Langmuir and freundlich adsorption isotherms fitted

c. Effect of pH on Cd^{2+} adsorption

d. Effect of ion strength on adsorption of Cd^{2+} by biochar

e. Recyclability after six adsorption-desorption cyclc tests.

Figure 5 Experimental results of Cd^{2+} adsorption by biochar

Table 4 Adsorption kinetic model parameters of biomass carbon adsorption Cd^{2+}

Sample	Quasi-level			Quasi-secondary		
	Qe/(mg·g^{-1})	K_1/min^{-1}	R^2	Qe/(mg·g^{-1})	K_2/(mg·g^{-1}·h^{-1})	R^2
BC	43.80	0.049 33	0.907 69	45.85	0.001 13	0.952 94
AC	113.76	0.066 70	0.933 39	117.77	0.001 12	0.982 38
GO–AC	144.34	0.080 39	0.913 65	148.87	0.001 88	0.979 67

Table 5 Parameters related to Langmuir and Freundlich models

Sample	Langmuir			Freundlich		
	Q_m/ mg·g^{-1}	KL/ L·mg^{-1}	R^2	K_F/ mg·g^{-1}	n	R^2
BC	44.81	0.0222	0.9423	6.4770	3.0100	0.9184
AC	126.11	0.0233	0.9372	22.4396	3.1053	0.9063
GO-AC	169.96	0.0388	0.9749	44.8027	4.2803	0.9229

In the Freundlich model, the n-value can be used as an indicator of the strength of the adsorption[26]. From Table 5, it can be seen that the Freundlich model constant n values of Cd^{2+} in BC, AC, and GO–AC three biomass carbon adsorption solutions are 3.0100 and 3.1053, 4.2803 respectively, indicating that the adsorption process of metal ions and three kinds of biomass carbon is relatively easy to carry out. The larger the K_F value is, the better the adsorption performance, which shows that GO–AC has a stronger fixing ability of Cd^{2+}. The Freundlich model suggests that the interaction between Cd^{2+} and biochar adsorbents may be controlled primarily by multilayer chemical adsorption, and that adsorption is heterogeneous. Therefore, the adsorptions of Cd^{2+} reactions for the three kinds of biomass carbon are relatively easy to carry out, and the adsorption processes are performed at the same time.

3.3.3 Effects of pH on Cd^{2+} adsorption

The pH of the solution plays a significant role in the Cd^{2+} adsorption process by altering the surface charge of the biochar and hence the electrostatic interaction with Cd^{2+}. The effects of different pH conditions on biochar adsorption of Cd^{2+} are shown in Figure 5c. In the typical pH range, the adsorption capacities of Cd^{2+} are in the following order: GO–AC>AC>BC, indicating that the activation and loading of GO can enhance the efficiency of biochar's adsorption.

As observed in the image, the pH of the solution has a considerable impact on biochar's adsorption to bind Cd^{2+}, and when the pH value is 6, the adsorption effect of biochar on Cd^{2+} is the best, and the adsorptions of BC, AC and GO–AC is 45.16 mg/g, 119.21 mg/g, and 155.96 mg/g, respectively. With the decrease in pH, the adsorption amount of biochar also shows a gradually

decreasing trend, and the adsorption amount reaches its lowest value at pH 2 because of the increased concentration of H^+ in the solution under the low pH conditions; the same phenomenon occurs with Cd^{2+}. Competition develops, and the hydrated ion radius of H^+ is smaller than the hydrated ion radius of Cd^{2+}, so H^+ is relatively easier to adsorb than Cd^{2+} by biochar, thereby occupying the adsorption site and inhibiting the adsorption of Cd^{2+}. Increasing gradually as the solution's pH, the H^+ concentration decreases, the negative charge on the biochar surface increases, and the electrostatic gravitational attraction of Cd^{2+} and the biochar surface also increases. When the solution's pH is high (pH>6), Cd^{2+} is susceptible to hydrolysis, generating $Cd(OH)_2$ precipitation. Thus, a decrease in the adsorption effect at a pH of 7 and 8 can be attributed to ash and alkaline substances being desorbed from the surface of the adsorbent, increasing pH as a result and the formation of $Cd(OH)_2$ from the precipitate, thereby reducing the content of removable Cd^{2+} in the solution.

3.3.4 Effect of ionic strength on the adsorption of Cd^{2+}

The actual composition of wastewater containing heavy metals is more complex, and other electrolyte ions may coexist with Cd^{2+} that can impact the adsorption of Cd^{2+} by affecting the effectiveness of heavy metal adsorption sites on the surface of biochar. The effect of ionic strength on Cd^{2+} adsorption is shown in Figure 5d, and with increasing NaCl concentration, the three biochars are affected regarding their adsorption of Cd^{2+}. The volume shows a trend of first rising and then gradually decreasing. This could be due to three reasons:

(1) Under the action of static electricity, the low concentrations of NaCl formed a double electron layer structure around the Cd^{2+} adsorbed on the surface of biochar, which was conducive to the adsorption of Cd^{2+} by biochar. (2) With increasing NaCl concentration, the repulsion force between the two electron layers decreased while the van der Waals force remained unchanged, weakening the electrostatic interaction between the surface charge of biochar and the heavy metals in solution and reducing the effective collision and contact between Cd^{2+} and biochar. (3) In solution, Na^+ and Cd^{2+} compete for adsorption sites, and the hydrated cation radius of Na^+ was lower than that of Cd^{2+}, which is more likely to occupy the adsorption site than Na^+. Additionally, the results show the Cd^{2+} sorption process of GO–AC is a combination of chemical and physical adsorption. When the concentration of NaCl was 1 mol/L, adsorption of Cd^{2+} by BC, AC, and GO–AC biochar was reduced by 33.7%, 27.76%, and 21.79%, respectively, indicating that GO–AC has higher applicability for ion strength.

3.3.5 Recycling experiments

Due to the strict ecological and economic requirements for sustainability, the assessment of adsorbent regeneration is of great significance for practical applications[27]. The regenerative performances of BC, AC, and GO-AC on Cd^{2+} adsorption were evaluated through six cyclic adsorption experiments, and the results are shown in Figure 5e. From Figure 5e, it can be seen that the adsorption capacity of Cd^{2+} on the three biochars gradually decreased in six adsorption/desorption cycles and finally stabilized, and the adsorption capacities on BC, AC, and GO–AC were stable at approximately 42.47%, 38.69%, and 57.23%, respectively. The decrease in adsorption could be attributed to the partial desorption of Cd^{2+} adsorbed on the surface of biochar by electrostatic forces; the Cd^{2+} is not completely desorbed by HCl as π-π bonding, hydrogen bonding, and oxygen-containing functional group actions, resulting in a reduced adsorption capacity of the sample. Furthermore, the adsorption of Cd^{2+} by GO–AC after six adsorption-desorption cycle tests was still as high as 89.26 mg/g, which was 93.5% and 365% greater than the adsorption amount of BC (19.18 mg/g) and AC (46.13 mg/g), respectively, after six adsorption-desorption cycle tests, which proved that GO–AC had good reuse performance.

3.4 Discussion of adsorption mechanisms

Using biochar made from cow dung, sludge, and peanut shells, heavy metals have been demonstrated to be adsorbed in some investigations. It was shown that the heavy metals might attach to the mineral fraction on the surface of the biochar and eventually be removed in the form of sedimentation. Zhang et al. used biochar prepared from poplar sawdust to adsorb Cd^{2+} from water bodies and found that Cd^{2+} was removed as $Cd(OH)_2$ precipitation[28]; Cui et al. showed that the adsorption of heavy metal Cd^{2+} by cattle manure biochar is mainly the formation of phosphate or carbonate precipitation[29]. In this study, GO-AC modified biomass carbon showed strong adsorption capacity in the adsorption of heavy metal Cd^{2+}, and XPS confirmed the production of $Cd(OH)_2$ and $CdCO_3$, indicating that precipitation is one of the key mechanisms for Cd^{2+} adsorption by GO-AC.

Cao et al. suggested that a large number of alkaline cations were released during the adsorption of heavy metals from biochar, leaving the adsorption sites on the surface of biochar vacant, and heavy metal ions exchanged with the released cations and adsorbed on the vacant sites[30]. The Oxygenated functional groups (for example -OH and -COOH) on the biochar surface can chelate with heavy metal ions to achieve adsorption purposes and immobilization of heavy metals. The inorganic salt ions (Ca^{2+}, Mg^{2+}, K^+, and Na^+, etc.) or some functional groups (-COOM and -R-O-M, etc.) in biochar can exchange ions with heavy metal ions, thus removing heavy metal ions[31]. In this study, it was found that during heavy metal adsorption, a large number of basic cations contained in GO-AC were released, and ion exchange interaction with Cd^{2+} occurred thus achieving the removal of heavy metal Cd. Similarly, Qian et al. and Hsu et al. prepared biochar with peanut shells for the removal of mercury with similar cation exchange[32,33]. In terms of functional group chelation, the FTIR spectra and amount of change of functional groups after adsorption and before indicated that GO-AC had more oxygenated functional groups compared with AC, and the oxygenated functional groups might have participated in the complexation and adsorption process of biochar on heavy metals.

Peng et al. and Wu et al. found that unsaturated structures such as aromatic rings and C=C on the surface of biochar generate a large number of π electrons, which can bind to heavy metal ions through coordination bonding, thus achieving their immobilization or removal[34,35]. The FTIR spectrum of this study showed that the adsorption of heavy metals by GO-AC resulted in a significant shift of its absorption peak due to the cation-π chelation effect, which exhibited a distinct aromatic ring characteristic functional group. Similarly, Liao et al. and Bao et al. found that cation-π chelation plays an active role in the biochar's adsorption of heavy metals[18,36].

The composites in this study exhibit similar adsorption mechanisms to those prepared by previous authors, suggesting that the main mechanisms of adsorption of heavy metals include (Figure 6): (1) Precipitation, mainly carbonate precipitation ($CdCO_3$) formed by inorganic mineral ions (CO_3^{2-}) and heavy metal ions (Cd^{2+}) in biochar ash and $Cd(OH)_2$ precipitation formed by OH^- and Cd^{2+}. (2) Functional group chelation, mainly the formation of chelates between oxygen-containing functional factors in biochar (-OH and -COOH, etc.) and heavy metal ions; (3) Ion exchange, mainly inorganic salt ions (K^+ and Na^+, etc.) or some functional

groups (-COOH and -OH, etc.) in biochar are removed by ion exchange with Cd^{2+}; (4) Cd^{2+}-π chelation, where π electrons in biochar (C-C and C=C, etc.) interact with heavy metal ions through ligand bonding, resulting in adsorption of heavy metal ions.

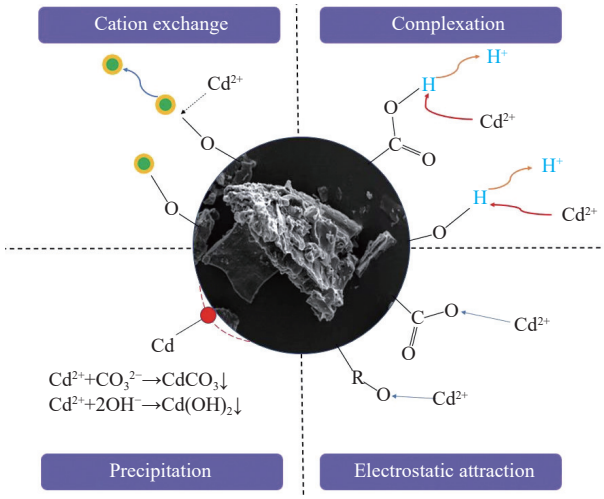

Figure 6 The mechanistic model of Cd^{2+} adsorption process on GO-AC

4 Conclusions

(1) By comparison of adsorption experiments, GO-AC has higher adsorption efficiency and adsorption capacity, and the maximum adsorption amount of Cd^{2+} (155.96 mg/g) is 3.45 and 1.30 times higher than that of BC (45.16 mg/g) and AC (119.21 mg/g), respectively, and the adsorption capacity is increased by 245.3% and 30.8%, respectively.

(2) The characterization results showed that GO-AC has more micropores and larger specific surface area, more surface adsorption sites and more oxygen-containing functional groups than BC and AC. GO-AC is mainly used for the removal of Cd^{2+} from aqueous solution by complexation of surface functional groups (e.g. -OH, -COOH, etc.) with Cd^{2+} and surface adsorption at the same time. The adsorption process is mainly chemisorption, and physical and chemical adsorption coexist, and the adsorption is non-homogeneous, and the adsorption process is carried out simultaneously in single and double layers.

(3) The adsorption amount of Cd^{2+} by GO-AC was still as high as 89.26 mg/g after six adsorption-desorption cycles, which was still 93.5% and 365% higher than that of BC (19.18 mg/g) and AC (46.13 mg/g), respectively, which proved the good reusability of GO-AC.

Acknowledgements

This work was supported by the National Natural Science Foundation of China (41201224); Postgraduate Education Reform Project of Henan Province(2021SJGLX138Y); Henan Province Science and Technology Research Project (192102110050); Project for the Training of Young Backbone Teachers of Higher Education Institutions in Henan Province (2018GGJS047).

[References]

[1] Sall M L, Diaw A K D, Gningue-Sall D, Efremova Aaron S, Aaron J-J. Toxic heavy metals: impact on the environment and human health, and treatment with conducting organic polymers, a review. Environ Sci Pollut Res, 2020; 27(24): 29927–29942.

[2] Inyang M I, Gao B, Yao Y, Xue Y, Zimmerman A, Mosa A, et al. A review of biochar as a low-cost adsorbent for aqueous heavy metal removal. Crit Rev Env Sci Tec, 2016; 46(4): 406–433.

[3] Yadav S, Yadav A, Bagotia N, Sharma AK, Kumar S. Adsorptive potential of modified plant-based adsorbents for sequestration of dyes and heavy metals from wastewater: A review. J Water Process Eng, 2021; 42: 352–365

[4] Issaka E, Fapohunda F O, Amu-Darko J N O, Yeboah L, Yakubu S, Varjani S, et al. Biochar-based composites for remediation of polluted wastewater and soil environments: Challenges and prospects. Chemosphere, 2022; 297: 134163.1–134163.14

[5] Liu C, Zhang H X. Modified-biochar adsorbents (MBAs) for heavy-metal ions adsorption: A critical review. J Environ Chem Eng, 2022; 10(2): 107393.

[6] Sessa F, Merlin G, Canu P. Pine bark valorization by activated carbons production to be used as VOCs adsorbents. Fuel, 2022; 318: 123346.1–123346.10

[7] Herath A, Layne C A, Perez F, Hassan E I B, Pittman C U, Mlsna T E. KOH-activated high surface area Douglas Fir biochar for adsorbing aqueous Cr(VI), Pb(II) and Cd(II). Chemosphere, 2021; 269: 128409. 107–121

[8] Liew R K, Azwar E, Yek P N Y, Lim X Y, Cheng C K, Ng J-H, et al. Microwave pyrolysis with KOH/NaOH mixture activation: A new approach to produce micro-mesoporous activated carbon for textile dye adsorption. Bioresource Technol, 2018; 266: 1–10.

[9] Duan C, Ma T, Jianyu W. Removal of heavy metals from aqueous solution using carbon-based adsorbents: A review. J Water Process Eng, 2020; 37: 101339.

[10] Liu J, Jiang J, Meng Y, Aihemaiti A, Xu Y, Xiang H, et al. Preparation, environmental application and prospect of biochar-supported metal nanoparticles: A review. J Haz Mat, 2020; 388: 122026.

[11] Oliveira F R, Patel A K, Jaisi D P, Adhikari S, Lu H, Khanal S K. Environmental application of biochar: Current status and perspectives. Bioresource Technol, 2017; 246: 110–22.

[12] Khabibrakhmanov A I, Sorokin P B. Electronic properties of graphene oxide: nanoroads towards novel applications. Nanoscale, 2022; 14(11): 4131–4144.

[13] Tian Y, Yu Z, Cao L, Zhang X L, Sun C, Wang D-W. Graphene oxide: An emerging electromaterial for energy storage and conversion. J Energy Chem, 2021; 55: 323–344.

[14] Dhamodharan D, Ghoderao PP, Dhinakaran V, Mubarak S, Divakaran N, Byun H-S. A review on graphene oxide effect in energy storage devices. J Ind Eng Chem, 2022; 106: 20–36.

[15] Yu H, Hong H-J, Kim S M, Ko H C, Jeong H S. Mechanically enhanced graphene oxide/carboxymethyl cellulose nanofibril composite fiber as a scalable adsorbent for heavy metal removal. Carbohyd Polym, 2020; 240: 116348.

[16] Arvas M B, Gürsu H, Gencten M, Sahin Y. Preparation of different heteroatom doped graphene oxide based electrodes by electrochemical method and their supercapacitor applications. J Energy Storage, 2021; 35: 239–249.

[17] Liu H, Liu X, Zhao F, Liu Y, Liu L, Wang L, et al. Preparation of a hydrophilic and antibacterial dual function ultrafiltration membrane with quaternized graphene oxide as a modifier. J Colloid Interf Sci, 2020; 562: 182–92.

[18] Bao S, Yang W, Wang Y, Yu Y, Sun Y. One-pot synthesis of magnetic graphene oxide composites as an efficient and recoverable adsorbent for Cd(II) and Pb(II) removal from aqueous solution. J Haz Mat, 2020; 381: 120914.

[19] Jr W, Offeman R E. Preparation of graphitic oxide. J Am Chem Soc, 1958; 80(6): 1339–1446

[20] Padmarajan N, Selvaraj S K. Sig sigma implementation (DMAIC) of friction welding of tube to tube plate by external tool optimization. Materials Today:Proceedings, 2021; 46: 7344–7350.

[21] Feng D, Guo D, Zhang Y, Sun S, Zhao Y, Shang Q, et al. Functionalized construction of biochar with hierarchical pore structures and surface O-/N-containing groups for phenol adsorption. Chem Eng J, 2021; 410: 127707.2–12

[22] Liu C, Ye J, Lin Y, Wu J, Price G W, Burton D, et al. Removal of Cadmium (II) using water hyacinth (*Eichhornia crassipes*) biochar alginate beads in aqueous solutions. Environ Pollut, 2020; 264: 114785.1–114785.9

[23] Thulasiram R, Murugan S, Ramasamy D, Sundaramoorthy S. Modelling and evaluation of combustion emission characteristics of COME biodiesel

using RSM and ANN—a lead for pollution reduction. Environ Sci Pollut Res, 2021; 28(26): 34730–41.

[24] Li H, Dong X, da Silva EB, de Oliveira LM, Chen Y, Ma LQ. Mechanisms of metal sorption by biochars: Biochar characteristics and modifications. Chemosphere, 2017; 178: 466–478.

[25] Zhao G, Li J, Ren X, Chen C, Wang X. Few-layered graphene oxide nanosheets as superior sorbents for heavy metal ion pollution management. Environ Sci & Technol, 2011; 45(24): 10454–10462.

[26] Araújo C S T, Almeida I L S, Rezende H C, Marcionilio S M L O, Léon J J L, de Matos T N. Elucidation of mechanism involved in adsorption of Pb(II) onto lobeira fruit (*Solanum lycocarpum*) using Langmuir, Freundlich and Temkin isotherms. Microchem J, 2018; 137: 348–354.

[27] Ahmad M, Rajapaksha A U, Lim J E, Zhang M, Bolan N, Mohan D, et al. Biochar as a sorbent for contaminant management in soil and water: A review. Chemosphere, 2014; 99: 19–33.

[28] Zhang L, Zhang Y, Huang Y, Han G, Sana H, Su S, editors. Cadmium (II) removal from aqueous solution by magnetic biochar composite produced from KOH-modified poplar sawdust biochar. TMS 1st Annual Meeting & Exhibition Supplemental Proceedings, 2022, Cham: Springer International Publishing, 2022; 155st: 807–816

[29] Cui X, Wang J, Wang X, Du G, Khan K Y, Yan B, et al. Pyrolysis of exhausted hydrochar sorbent for cadmium separation and biochar regeneration. Chemosphere, 2022; 306: 135546.

[30] Cao B, Qu J, Yuan Y, Zhang W, Miao X, Zhang X, et al. Efficient scavenging of aqueous Pb(II)/Cd(II) by sulfide-iron decorated biochar: Performance, mechanisms and reusability exploration. J Environ Chem Eng, 2022; 10(3): 107531.

[31] Chen Y, Li M, Li Y, Liu Y, Chen Y, Li H, et al. Hydroxyapatite modified sludge-based biochar for the adsorption of Cu^{2+} and Cd2+: Adsorption behavior and mechanisms. Bioresource Technol, 2021; 321: 124413.

[32] Hsu C-J, Cheng Y-H, Huang Y-P, Atkinson J D, Hsi H-C. A novel synthesis of sulfurized magnetic biochar for aqueous Hg(II) capture as a potential method for environmental remediation in water. Sci Total Environ, 2021; 784: 147240.

[33] Qian X, Wang R, Zhang Q, Sun Y, Li W, Zhang L, et al. A delicate method for the synthesis of high-efficiency Hg (II) the adsorbents based on biochar from corn straw biogas residue. J Clean Prod, 2022; 355: 131819.1–131819.10

[34] Peng B, Liu Q, Li X, Zhou Z, Wu C, Zhang H. Co-pyrolysis of industrial sludge and rice straw: Synergistic effects of biomass on reaction characteristics, biochar properties and heavy metals solidification. Fuel Process Technol, 2022; 230: 107211.

[35] Wu J, Wang T, Shi N, Pan W-P. Insight into mass transfer mechanism and equilibrium modeling of heavy metals adsorption on hierarchically porous biochar. Sep Purif Technol, 2022; 287: 120558.

[36] Liao J, Xiong T, Ding L, Zhang Y, Zhu W. Effective separation of uranium (VI) from wastewater using a magnetic carbon as a recyclable adsorbent. Sep Purif Technol, 2022; 282: 120140.